

Quantum well and resonance-band split off in a K monolayer on Cu(111)

F. Schiller,¹ M. Corso,² M. Urdanpilleta,¹ T. Ohta,³ A. Bostwick,³ J. L. McChesney,³ E. Rotenberg,³ and J. E. Ortega^{1,2}

¹*Departamento de Física Aplicada I, Universidad del País Vasco, Plaza Oñate 2, E-20018 San Sebastián, Spain*

²*Donostia International Physics Center and Centro Mixto de Materiales CSIC/UPV, Paseo Manuel Lardizabal 4, E-20018 San Sebastián, Spain*

³*Advanced Light Source, Lawrence Berkeley National Laboratory, Berkeley, California 94720, USA*

(Received 13 February 2008; published 25 April 2008)

The potassium monolayer on Cu(111) defines the simplest metallic quantum well that confines a single s -like discrete level. The analysis of the metallization onset in such a K adlayer reveals, however, a subtle electronic structure. The metallic monolayer condensate is actually characterized by a pair of two-dimensional states that lie below the Fermi energy, namely, a quantum well state and a resonant band reminiscent of the Cu(111) surface state. All quantum well states, resonances, and Cu substrate bulk bands exhibit smooth K coverage dependence, suggesting that changes in the crystal potential upon K adsorption extend from the surface and/or interface inside the Cu substrate.

DOI: [10.1103/PhysRevB.77.153410](https://doi.org/10.1103/PhysRevB.77.153410)

PACS number(s): 73.20.-r, 73.21.-b, 79.60.Dp

Quantum well (QW) states of thin metal films and multilayers are of fundamental interest in present and future technology applications. Over the past few years, a number of metallic QW systems have been grown with a high degree of interface and thickness perfection. This allows the discovery of exotic energy and structure interplay phenomena, such as the so-called quantum growth,¹ or to unveil the role of the electronic and geometric properties of the substrate in the spectrum of QW levels.^{2,3} The latter is of particular importance because, in the end, the exotic properties in metallic QWs, such as the spin polarization in nonmagnetic films,⁴ are the direct consequence of QW scattering at the interface, which in turn opens the way to new applications through interface engineering.^{3,5}

Alkali metal films on noble metal substrates of the (111) orientation, such as Cu(111), are prototypes of metallic quantum wells with s -like electrons confined by a substrate bulk gap. On the other side, the alkali monolayer is a model QW with a single s -like level. The alkali/Cu(111) system is very suitable to track the evolution of electronic states from the low-density, adsorbed-atom phase, with ionic bonding with the surface, to a more condensed phase near monolayer completion, with metallic bonds inside alkali islands (metallic condensation). The monolayer growth on Cu(111) has a rich structural behavior,⁶ which is indeed reflected on the electronic structure.⁷⁻¹² For very small coverage, the Shockley state of the clean Cu(111) surface survives but shifts down in energy. As coverage increases, the surface state is pushed beyond the bulk band gap and inside the bulk continuum. At the same time, the work function decreases and the unoccupied image state shifts toward the Fermi energy. At a coverage of 0.6–0.8 ML (monolayer), the alkali metal condenses into monolayer thick islands, and the image state smoothly drops below E_F , transforming into the characteristic QW state of the alkali metal overlayer.^{9,12} At a full monolayer coverage, angle resolved photoemission shows a parabolic QW band with a relatively large effective mass compared to the Cu(111) surface state ($0.8m_e$ vs $0.41m_e$) located 135 meV below the Fermi energy for Li,¹⁰ 127 meV for Na,¹¹ 100 meV for K,⁸ and 25 meV for Cs.¹²

Despite its simplicity, the alkali/Cu(111) system exhibits

subtle properties that break the simple picture of the totally confined QW state.^{12,13} The alkali layer and the Cu substrate possess different lattice constants, such that an effective overlap with bulk states may actually occur via umklapp with reciprocal superlattice vectors.¹³ On the other hand, finite size gaps lead to a considerable penetration of the QW wave function inside the substrate crystal, and hence QW electronic states must exhibit both substrate and overlayer lattice properties. This double substrate and adlayer periodicity explains the presence of an extra resonant state in first principles calculations.¹² Here, we present the experimental evidence of this QW/resonance split off that defines the K/Cu(111) monolayer. We observe that the resonant state evolves from the clean surface state, but it only becomes a strong feature in the metallic condensate phase and close to the Fermi energy. The photoemission intensity reflects a rapid spectral density variation across the surface Brillouin zone, which is explained as connected to the wave function properties of the resonant state.¹² Finally, we observe that not only the alkali metal layer states (QW and resonance) but also bulk states display a smooth transformation upon the monolayer completion, proving that the adlayer affects the crystal potential deep inside the Cu substrate.

The photoemission experiments have been performed at beamline 7.0.1 of the Advanced Light Source at the Lawrence Berkeley Laboratory by using a hemispherical Scienta R4000 spectrometer and p -polarized photons of energies $h\nu=80$ eV and $h\nu=105$ eV. Energy and angular resolutions were set to 25 meV and 0.1° , respectively. We used a cylindrical Cu crystal with a smooth $\pm 15^\circ$ miscut variation with respect to the (111) direction. Such a curved surface opens the possibility to study the influence of the steps on the electronic states of the K adlayer. The small spot size (below 100 μm) allowed scanning of the x-ray beam on the surface and hence selecting the appropriate crystal orientation. Such a curved surface is cleaned with standard sputtering-annealing cycles, after which it exhibits a sharp low energy electron diffraction pattern, with a smoothly varying spot splitting away from the (111) orientation. In order to ensure surface diffusion and homogeneous layer formation, the K adsorption is done at 300 K, with the (111) plane placed

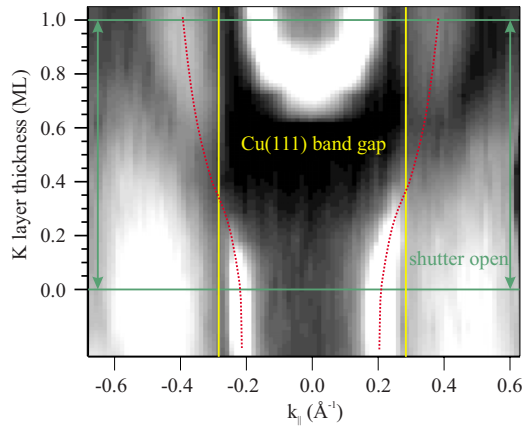


FIG. 1. (Color online) Fermi surface cut along the $\bar{\Gamma}\bar{M}$ direction as a function of K coverage. The vertical lines mark the edge of the projected band gap in Cu(111). The low coverage regime is characterized by the transformation of the Cu(111) surface state into a weak resonance, mostly quenched at 0.5 ML. Upon metallic condensation, the QW band shifts below the Fermi energy and the resonant emission strongly picks up (dotted line).

at the focus of the analyzer. Thus, thickness-dependent K/Cu(111) photoemission spectra could be recorded while the evaporation was performed, as shown in Fig. 1. The ML is defined as the coverage at which the QW energy reaches its maximum binding energy (see below).¹¹ Upon saturation with 1 ML, the crystal was quickly cooled down to 125 K.

Figure 1 shows the Fermi level intensity measured as a function of the K coverage along the $\bar{\Gamma}\bar{M}$ symmetry direction. The two intense maxima observed prior to K deposition at $\pm \sim 0.2 \text{\AA}^{-1}$ are the Fermi crossings of the Cu(111) Shockley surface state. The measurement reflects the smooth transformation of this surface state into a resonance and the appearance of the double resonant/QW band at the onset of the K metallic condensation. The evaporation rate is 0.07 ML/min, such that a single spectrum was recorded every 0.025 ML step. The evolution of the different features is better understood in the light of Figs. 2(a)–2(c), where we show the band dispersion in the light of Figs. 2(a)–2(c), where we show the band dispersion for the clean surface, 0.4 and 1 ML. In order to enhance the resonant state in both Figs. 1 and 2, the intensity scale is saturated in the QW and the Cu surface state. A more accurate quantitative photoemission intensity variation of the surface resonance is shown in Fig. 3. Coming back to Fig. 1, we can clearly observe that the Cu(111) surface state smoothly shifts toward the edge of the gap (vertical lines in Fig. 1) as the coverage increases, overlapping with the continuum of bulk bands and getting almost quenched at ~ 0.5 ML. It is known that the K QW band crosses E_F when the K layer becomes a metallic condensate around ~ 0.7 ML.^{8,9} In Fig. 1, we also show that, at the same time, a second emission emerges outside of the copper band gap. This K ML resonance appears to evolve (dotted line) from the surface state, although it only strongly builds up upon metallic condensation. The critical coverage for the resurgence of the resonance and the crossing of the QW band across E_F is 0.75 ML, as carefully determined in Fig. 3(a). Assuming a 4.4\AA lattice constant for the 1 ML condensate,⁶ the critical 0.75 ML coverage corresponds to a 5.08\AA K

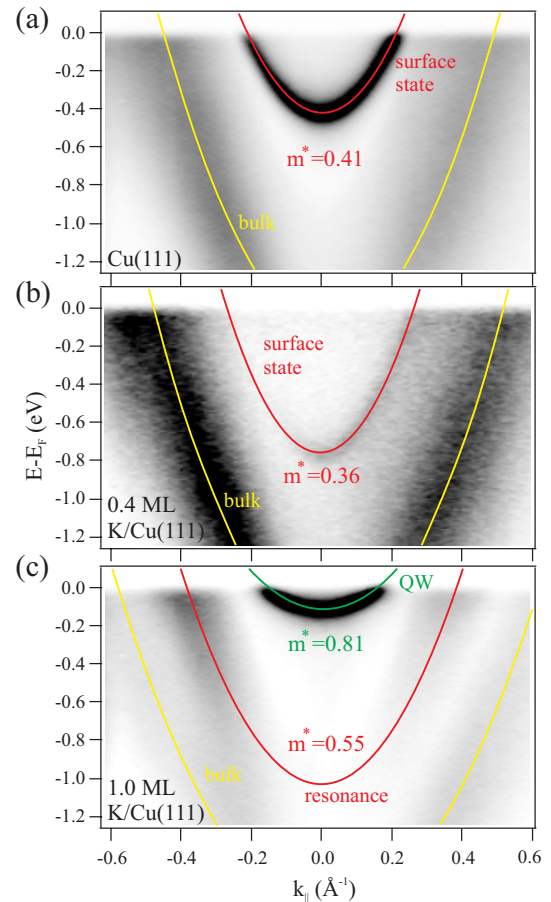


FIG. 2. (Color online) K QW band, surface states and resonances, and Cu bulk bands for (a) Cu(111), (b) 0.4 ML K/Cu(111), and (c) 1 ML K/Cu(111). The photon energy is 80 eV. All surface and bulk bands exhibit coverage-dependent shifts, suggesting that K adsorption affects the crystal potential not only at the surface but also inside the substrate.

adatom lattice, i.e., to the (2×2) commensurate reconstruction of the copper substrate with lattice constant $a = 3.605 \text{\AA}$. Therefore, three features, namely, the (2×2) overlayer arrangement, the QW Fermi level crossing, and the resonance, characterize the metallic condensation of K on Cu(111).

Thin lines in Fig. 2 represent parabolic fits to the different bands after separate analysis of individual spectra. The surface state evolves from $E_0 = -0.41 \text{ eV}$ and $m^* = 0.41m_e$ in the clean surface to $E_0 = -0.755 \text{ eV}$ and $m^* = 0.36m_e$ for the 0.4 ML surface resonance and to $E_0 = -1.03 \text{ eV}$ and $m^* = 0.55m_e$ in the strong split off K ML resonance. The latter values are similar to the energy and the effective mass predicted for the (2×2) Cs layer on Cu(111),¹² indicating the same physical nature in both K and Cs ML resonances. Similarly, the K ML QW state values $E_0 = -0.11 \text{ eV}$ and $m^* = 0.81m_e$ agree with data on Na metallic monolayers [$E_0 = -0.127 \text{ eV}$, $m^* = 0.7m_e$ (Ref. 11)]. On the other hand, note that the bulk sp band (low energy parabola) smoothly shifts down from Cu(111) to the K covered substrate. The downshift behavior in both the QW state and the resonance can be explained as due to an increasingly attractive (average) crys-

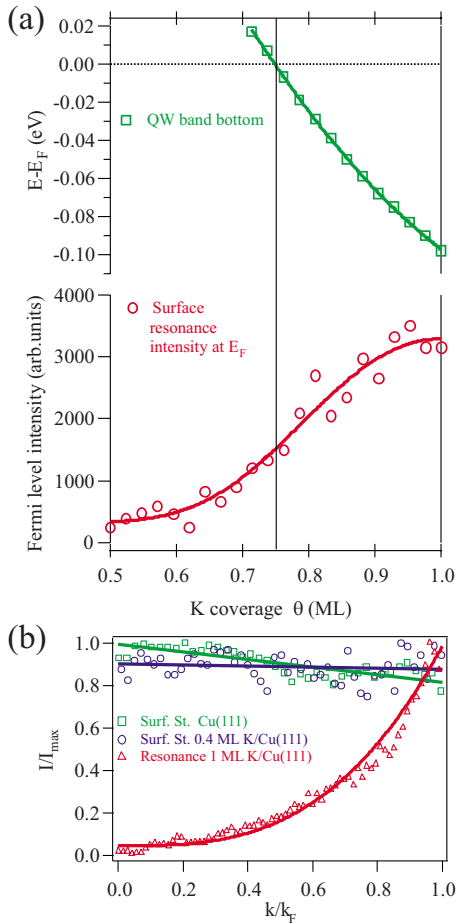


FIG. 3. (Color online) (a) Band bottom position of the K QW and intensity variation of the K ML resonance near metallic condensation (dotted line in Fig. 1) vs coverage. (b) Normalized photoemission intensity for the Cu surface state, the 0.5 ML K covered surface state, and the K ML resonance as a function of k_{\parallel} . A strong variation is observed for the K ML resonance, as expected from the wave function properties (see the text).

tal potential V_0 . Thus, a downward shift of the bulk sp band in Fig. 2 indicates that changes in V_0 extend to the bulk crystal at least within the sampling depth of the photoemission experiment. This could, in turn, be related to the presence of a substrate rumpling, which is found in the K/Al(111) and Cs/Al(111) systems¹⁴ and suggested in Na/Cu(111).¹⁵

In Fig. 2, we observe a strong k_{\parallel} dependence of the intensity in the K ML resonance band, exhibiting negligible emission at the band center and maximum intensity at E_F . Such dependence contrasts with the much weaker variation of the Cu surface state in the clean and the 0.4 ML covered surface, as depicted in Fig. 3(b). The strong k_{\parallel} dependence of the K ML resonance can be traced to the qualitative variation of its wave function from bulklike (lower photoemission intensity) to thin-film-like (higher photoemission intensity) along $\bar{\Gamma}\bar{M}$, as predicted for the Cs (2×2) metallic condensate in theoretical calculations.¹² At $\bar{\Gamma}$, the electron probability uniformly extends inside the bulk crystal, with a relatively low weight in the surface plane. In contrast, close to E_F , the

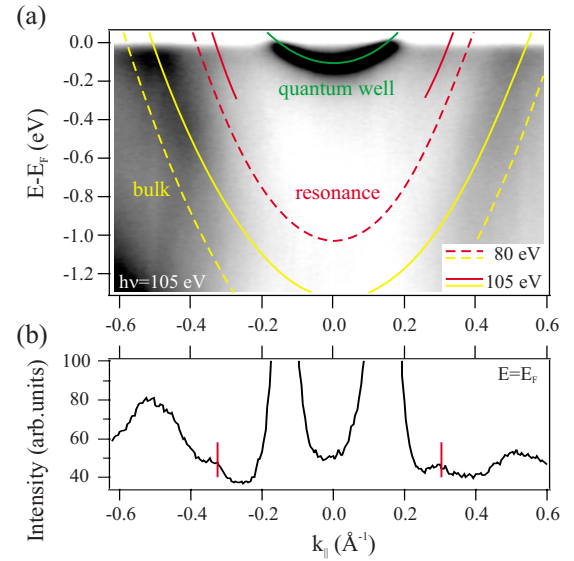


FIG. 4. (Color online) (a) Band dispersion and (b) photoemission intensity at the Fermi energy for the K monolayer measured at $h\nu=105$ eV. Solid lines are parabolic fits to the data, and dashed lines represent the same bands measured at $h\nu=80$ eV (extracted from Fig. 2). The two vertical lines in (b) mark the Fermi level crossings of the K resonance.

spatial variation of the wave function of the K ML resonance is similar to that of the QW state, i.e., a maximum probability at the K layer and a strong damping toward the bulk.

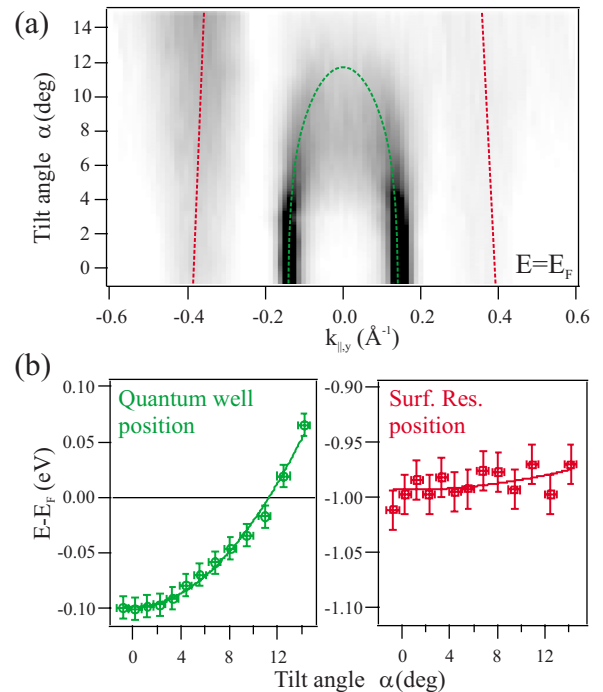


FIG. 5. (Color online) (a) Cut through the Fermi surface at $k_{\parallel,x}=0$ as a function of the tilt angle α and the wave vector $k_{\parallel,y}$, with $k_{\parallel,y}=0$ being the symmetry center perpendicular to the steps. (b) QW (left) and resonance (right) band bottom energies as a function of the orientation of the substrate with respect to the (111) direction. The measurements have been done at $h\nu=80$ eV and by scanning the photon beam across a cylindrical crystal.

The surfacelike and bulklike character of the K ML QW and resonance bands, respectively, is further probed in Fig. 4, where we test the photon energy dependence. On top, we show the 1 ML bands measured with $h\nu=105$ eV (marked by solid lines), which are compared to the bands extracted from Fig. 2 measured with $h\nu=80$ eV (dashed lines). By increasing the photon energy the QW remains unchanged, whereas the resonance and the copper bulk bands shift by 0.28 and 0.4 eV, respectively, as expected for bulklike bands with k_{\perp} dispersion. For the higher photon energy (105 eV), the K resonance band loses intensity and is only observed at energies close to the Fermi energy [see Fermi level crossings in Fig. 4(b)].

In Fig. 5, we show the evolution of the quantum well and the K resonance as a function of the surface orientation (tilt angle α) away from the (111) direction. Figure 5(a) is a cut through the Fermi surface with the wave vector perpendicular to the steps as a function of α , while Fig. 5(b) denotes the position of the QW and the resonance-band bottom energies. These data are taken in a straightforward way by scanning the beam across the cylindrical surface. Moving away from the (111) direction, we select substrate areas with an increasing density of steps. The QW exhibits an upward energy shift

as a function of this tilt angle, reflecting the repulsive electron scattering at step edges, which leads to a partial confinement within terraces of decreasing size.¹⁶ The ML resonance, in contrast, shows a negligible energy shift, as expected for a wave function with a significant weight in the bulk of the crystal and hence less sensitive to surface steps.

In summary, we have found the experimental evidence for the split off resonance predicted in metallic alkali monolayers on Cu(111). Such split off characterizes the K overlayer transformation from an ionic adsorbate to a metallic condensate at 0.75 ML. The bulk resonant character of the resonance state manifests in its photon energy dependence and its sensitivity to surface defects (steps). We also observe that Cu substrate bands, as K quantum well and resonant states, display coverage dependence, suggesting that changes in the crystal potential extend inside the bulk crystal.

Fruitful discussions with Slava Silkin are acknowledged. The work is supported through projects of the University of the Basque Country and the Basque Government (IT-257-07) and the Spanish Ministerio de Educacion y Ciencia (MAT2007-63083).

¹Z. Zhang, Q. Niu, and C. K. Shih, Phys. Rev. Lett. **80**, 5381 (1998); P. Czoschke, H. Hong, L. Basile, and T.-C. Chiang, *ibid.* **91**, 226801 (2003).

²L. Aballe, C. Rogero, P. Kratzer, S. Gokhale, and K. Horn, Phys. Rev. Lett. **87**, 156801 (2001); P. Moras, W. Theis, L. Ferrari, S. Gardonio, J. Fujii, K. Horn, and C. Carbone, *ibid.* **96**, 156401 (2006); N. Nagamura, I. Matsuda, N. Miyata, T. Hirahara, S. Hasegawa, and T. Uchihashi, *ibid.* **96**, 256801 (2006).

³D. A. Ricci, T. Miller, and T.-C. Chiang, Phys. Rev. Lett. **95**, 266101 (2005).

⁴J. E. Ortega and F. J. Himpsel, Phys. Rev. Lett. **69**, 844 (1992).

⁵W. Kuch, L. I. Chelaru, F. Offi, J. Wang, M. Kotsugi, and J. Kirschner, Nat. Mater. **5**, 128 (2006).

⁶R. D. Diehl and R. McGrath, Surf. Sci. Rep. **23**, 49 (1996).

⁷N. Fischer, S. Schuppler, R. Fischer, T. Fauster, and W. Steinmann, Phys. Rev. B **47**, 4705 (1993).

⁸N. Fischer, S. Schuppler, T. Fauster, and W. Steinmann, Surf.

Sci. **314**, 89 (1994).

⁹A. Carlsson, B. Hellsing, S. Å. Lindgren, and L. Walldén, Phys. Rev. B **56**, 1593 (1997).

¹⁰D. Claesson, S. Å. Lindgren, and L. Walldén, Phys. Rev. B **60**, 5217 (1999).

¹¹J. Kliewer and R. Berndt, Phys. Rev. B **65**, 035412 (2001).

¹²M. Breitholtz, V. Chis, B. Hellsing, S. Å. Lindgren, and L. Walldén, Phys. Rev. B **75**, 155403 (2007).

¹³C. Corriol, V. M. Silkin, D. Sánchez-Portal, A. Arnau, E. V. Chulkov, P. M. Echenique, T. von Hofe, J. Kliewer, J. Kröger, and R. Berndt, Phys. Rev. Lett. **95**, 176802 (2005).

¹⁴C. Stampfl, M. Scheffler, H. Over, J. Burchhardt, M. Nielsen, D. L. Adams, and W. Moritz, Phys. Rev. Lett. **69**, 1532 (1992); D. L. Adams, Appl. Phys. A: Mater. Sci. Process. **62**, 123 (1996).

¹⁵J. Kliewer and R. Berndt, Surf. Sci. **477**, 250 (2001).

¹⁶A. Mugarza and J. E. Ortega, J. Phys.: Condens. Matter **15**, S3281 (2003).